

STUDY OF THE DEVELOPMENT AND APPLICATION OF GLAZES OF A GLASS-CERAMIC NATURE WITH A VIEW TO ENHANCING THE TECHNOLOGICAL PROPERTIES OF CONVENTIONAL GLAZES.

M. Tichell(*), E. Fortanet(*), A. Pascual(*), J. Bakali(*)
G. Monrós(**), P. Escribano(**), J. B. Carda(**)

(*) ESMALTES S.A.

(**) Dept. of Organic and Inorganic Chemistry,
Universitat Jaume I de Castellón

ABSTRACT:

Through this study, glazes of a glass-ceramic nature have been obtained by introducing nucleating agents into a commercial boric crystalline frit, selected beforehand, studying the phenomena of nucleation and growth of zirconium silicate ($ZrSiO_4$) crystals in the industrial firing cycle of ceramic stoneware floor tiles, with a red as well as a white body, without altering these. Subsequently, in a second study stage, $\alpha-Al_2O_3$ crystals with preset characteristics were added to the glaze composition to obtain the glass-ceramic composite. The study of the presence of crystalline phases was carried out using X-ray diffraction and was completed using scanning electron microscopy and energy dispersive X-ray analysis (SEM/EDX). The mechanical properties of the materials obtained were also evaluated and their quality parameters determined.

Finally, the study on the glazed tile was completed with the development of a crystalline glass-ceramic for the screen-printing decoration and a granulated glaze, which had identical characteristics to the starting glaze, in order not to lose the improved mechanical properties obtained in the base glaze, during tile decoration.

1. INTRODUCTION

There is currently growing interest in the ceramic industry in this region in the development of new materials with better technological performance characteristics, centring on two variables: a greater refractive index in the glazes and improved mechanical strength⁽¹⁾. Nonetheless, the two parameters, gloss and hardness, would appear to be opposed. In this regard, new glazes with glass-ceramic characteristics could be designed and developed, which improve the mechanical properties of existing glazes and which in turn might keep an acceptable refractive index. This therefore involves developing "advanced glaze compositions and glaze coatings"⁽²⁾.

At the same time, there is a growing interest in the Spanish ceramic industry in environmental aspects, influenced on the one hand by the introduction of European regulations on the subject and on the other hand by the need to recycle industrial waste and to isolate toxic or hazardous waste, while at the same time achieving a potential economic saving⁽³⁾. In this field too, transformation of these raw materials - which in principle seem unusable, into new usable materials, may be of great use (4,5).

To start with, therefore, a glaze coating or ceramic glaze may be defined as glass that is applied to a ceramic body in order to protect or decorate the final ceramic product; glaze coatings or ceramic glazes are basically complex mixtures of silicates and or borates, basically formulated like glass with three types of component; glass-network forming oxides, modifying oxides and intermediate oxides⁽⁶⁾. For the production of glaze coatings or ceramic glazes, consequently, in order to prevent faults and to optimise or produce new products, phenomena such as immiscibility or nucleation and crystallisation, which are characteristic of glassy compositions, must be controlled⁽⁷⁾.

Controlling glass devitrification in order to produce a mainly crystallised material, is known as the "ceramming" process. Crystallisation of a glass may therefore be directed towards obtaining glass-ceramic materials with a given microstructure, which depends on the application required of the material obtained. One of the authors who has studied in greatest detail the glass-ceramic process is McMillan⁽⁸⁾, who establishes the following stages in the overall glass-ceramic process.

1) Fusion of a homogeneous glass, whose composition includes additives or constituents capable of producing nuclei for the development of crystallisation in a later process step.

2) Forming of the glass to give it a certain shape according to its service application.

3) Application of suitable heat treatments, to obtain an essentially crystalline material.

The heat treatments for crystallisation of the glass may be performed: either directly, in the cooling process, known as the “petrurgic” process, Fig. 1, or by first obtaining the glass at room temperature and later producing crystallisation by means of suitable heat treatments (“glass-ceramic process”), Fig. 2.

In the first case, a primary crystallisation would be obtained, producing what are known as petrurgic materials because of their similarity with natural processes of mineral genesis. In the second case, one speaks of secondary crystallisation and glass-ceramic materials.

Of the products obtained, generally those with the best properties are the ones in which a crystallisation of over 90% of the original glassy mass has been achieved, with a crystal size of between 0.5 and 1 μm . In order to achieve this, it is necessary on many occasions to use additives, particularly in processes with primary crystallisations, or in other words, in the petrurgic process.

Phase separation, which must sometimes be achieved for the production of glass-ceramic materials from silicate melts, arises when the glass contains cations whose coordination number varies with temperature, such as Ti, Zr, etc. or cations which contain a charge different to that of silicon and/or anions with a different charge to that of oxygen: Fe^{2+} , P^{5+} , F^- , or cations with a high field intensity, such as Cr^{3+} , Li^+ , Mg^{2+} , etc.

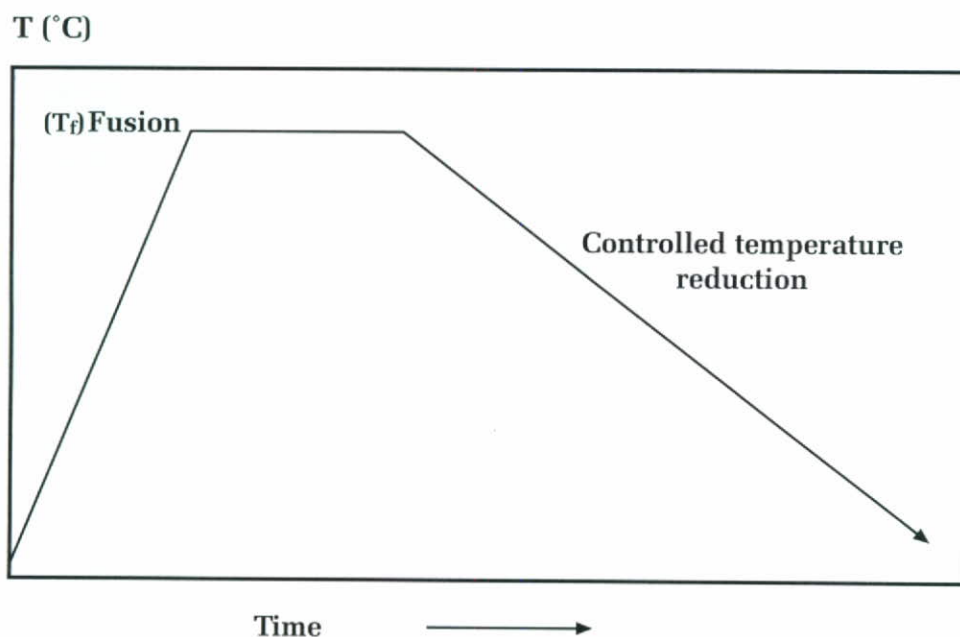


Figure 1.- Petrurgic process. Primary crystallisation in glass: glass obtention and subsequent heat treatments are included in a single cooling process ⁽⁹⁾

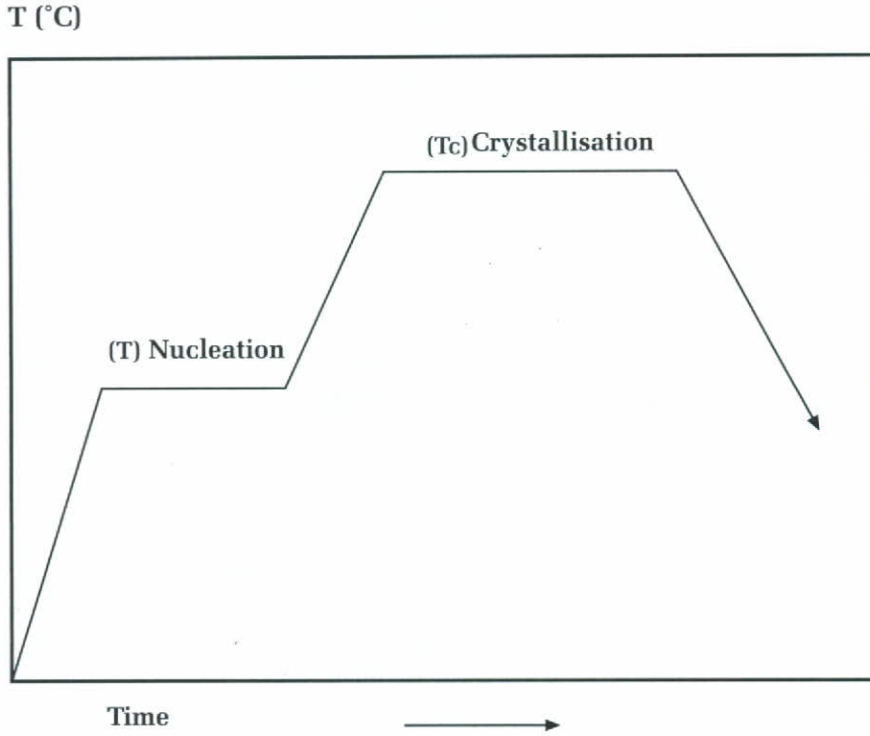


Figure 2.- Glass-ceramic process. Secondary crystallisation of glass: application of subsequent heat cycles different from those used in obtaining the glass⁽⁹⁾

There is a certain confusion in the denomination of the different glass-ceramic materials⁽¹⁰⁾. If one takes into account the process used in manufacturing these types of material, the petrurgic materials would only be those resulting from primary glass crystallisations, in which the heat treatments applied are included as an integral part of the cooling process; however, in a true glass-ceramic material, it is the result of provoking crystallisation of a previously obtained glass, by submitting it to subsequent heat treatments, regardless of the origin of the raw material.

On the other hand, because of the constant concern for achieving improvements in the mechanical strength of ceramic material, in view of its characteristic brittleness, new possibilities have opened up with the study and development of what have become known as structural ceramic materials, ceramic products of a passive character which basically function or serve in applied systems requiring high chemical resistance and thermo-mechanical strength. This is a new group of advanced ceramic materials which is currently being developed at great speed. The requirements for obtaining high performance (especially in mechanical properties) are as follows:

- a) high toughness at high and low temperatures.
- b) long average life, resistance to thermal shock.
- c) slow crack growth
- d) resistance to creep and corrosion.

As an example, Table 1 shows some of the properties of structural ceramic materials.

Table I. Properties of some structural ceramic materials.

Parameter	GLASS ⁽¹⁾	GLASS-CERAMIC	ZIRCON	COMPOSITES ⁽²⁾
Vickers Microhardness (Hv)	PbSi glass < 500 BSi, NaCa glass = 530 matt Zn = 600 matt Ba = 580	Pryoflan 660 Quartz 930	643-725	Norzon 14600 Cubitron 17900 Ni-alumina 21000
E (Pa)	BSi and Zn/Ba 70-50 steel 190 rubber 15 quartz 80	100	—	Norzon 200 Cubitron 350 Ni-alumina 362
σ_F (Mpa)	BSi glass 50-80	—	—	glass/alumina
K_{IC}	BSi glass 1.2 - 0.7 quartz 0.5 - 1 sapphire	2.5	1.3-5.0 ⁽³⁾	Norzon 4.5 Cubitron 6.0 Ni-alumina 4.6

- ⁽¹⁾ PbSi lead silicate glass. Matt Zn, matt zinc glaze
BSi borosilicate glass Matt barium glaze.
NaCa window glass.

⁽²⁾ Norzon nickel/zirconia commercial abrasives, Cubitron copper/zirconia

⁽³⁾ Depends heavily on the composition.

Thus, when hardening ceramic material, we can follow two possible routes: we may obtain composite materials or develop materials of a glass-ceramic nature. Composite ceramic materials are multiphase compatible materials, i.e. there exists the possibility of processing a material which is made up of a matrix which is the main material or phase and incorporating into it a second phase or various phases which, chemically, thermally and mechanically do not self-destruct or degrade, in other words, that are compatible.

From a mechanical point of view, ceramic materials are prepared with a view to optimising the mechanical resistance of the ceramic matrix. In accordance with Griffith's equation, there are two alternatives for improving the mechanical strength of a ceramic matrix: by ⁽¹¹⁾ incorporating a second phase with high K_{IC} or ⁽¹²⁾ having a microstructure with a small grain size. These alternatives can be suitably designed by using appropriate ceramic processing and it is now quite usual to employ continuous fibres with K_{IF} values of up to 15 Mpa·m as second phases. Nonetheless, it is also possible to use second phases with high Young's moduli as is the case with a composite material of a brittle matrix such as cubic zirconia and using a second phase with a high modulus, such as alumina. It may be shown experimentally that there is an important strengthening of the zirconia matrix at all testing temperatures when the proportion of alumina does not exceed 10% by weight. The same occurs with composite materials of tetragonal zirconia, where the positive influence of the alumina may be seen in the breaking value (Fig. 3). Composite materials of tetragonal zirconia with alumina percentages of between 10 and 20% by weight are known as *super-tough* materials. Such high K_{IC} and σ_F values are due to the special characteristics of their microstructure, and the constraint of the zirconia matrix by the presence of fine grains of alumina.

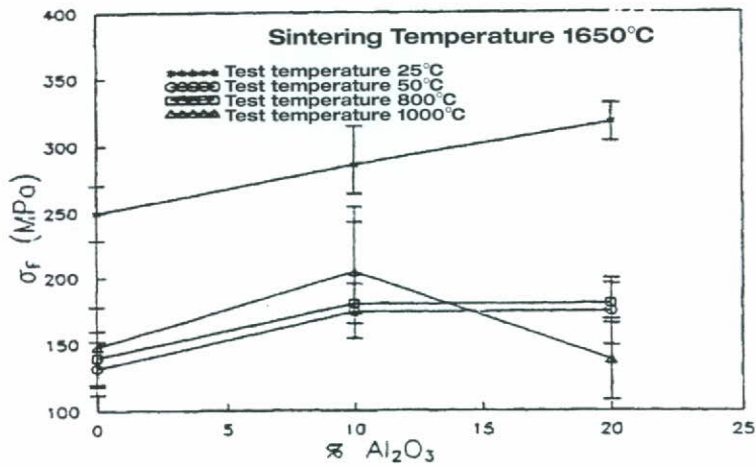


Figure 3. Graphic representation of the values of Young's modulus, σ_f , for a cubic zirconia, with the influence of the alumina addition, Al_2O_3 .

It should also be indicated that another characteristic of the influence that alumina has in the zirconia matrix, is the fact that the strengthening process also functions for crack deflection mechanisms, as shown in Fig. 4.

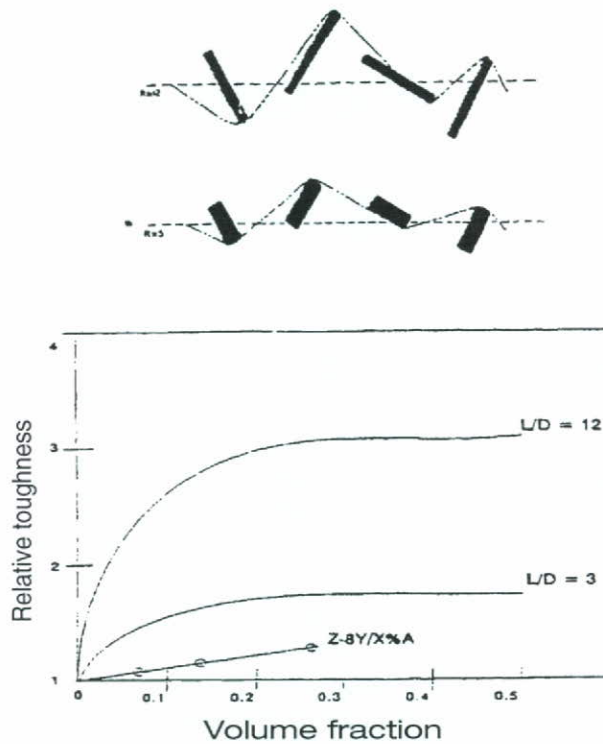


Figure 4. Influence of the length-diameter ratio of the dispersed particle on the strengthening of the matrix, proposed by Evans and Cannon.

At the same time, hardness is the term given to a material's resistance to the formation of surface tracks by an indenter under standard conditions. Depending on the application of this load there are three types of hardness: scratching, indentation and abrasion.

For example, a glass on the Mohs scale has a scratch hardness of between 5 and 6, but this scale of hardness is not the most suitable method of measuring the hardness of materials.

The most suitable method, especially for glass, is that of *microhardness* (H_v), which is the resistance offered by a material to the indentation produced when a concentrated load is applied to a small surface area. If a high load is applied to a glass using a pointed tip, a certain elastic deformation occurs as well as plastic flow. This flow seems to be due to Newtonian behaviour at high shear stresses, but there is a reduction in viscosity as load increases (this effect occurs because plastic deformation may be achieved). There is therefore a relationship between microhardness and viscosity, such that hardness increases with viscosity. When loading ceases, the glass undergoes partial elastic recovery, which varies inversely with the magnitude of the applied load. Interesting results have been obtained with glass:

- H_v increases when viscosity increases
- H_v falls according to modifier content, according to the sequence: CaO>MgO>BaO>PbO.
- H_v is greater for tempered glass than for annealed glass.
- H_v is higher for glass with slow cooling than for those obtained by quenching.

There are two methods for measuring microhardness: Vickers microhardness (H_v), which is the most widely used one in ceramic materials, and Knoop microhardness (H_k).

There can be no doubt that a basic requisite for characterisation of these types of material has been the parallel development of characterisation techniques. In this respect, electron microscopy, with its scanning (SEM) and transmission (TEM) variants, has proved to be a powerful technique, because of its high power of resolution. Furthermore, with the incorporation of energy dispersive X-ray analysis (EDX), it has become possible to characterise these materials quickly and accurately. This is therefore a technique of great interest, and rapid incorporation into the ceramic industry is anticipated because of the possibilities mentioned (13, 14).

As a result of the above, the company ESMALTES, S.A., together with the Materials Science research group from the Department of Organic and Inorganic Chemistry of the Universitat Jaume I, decided to attempt to develop composite glass-ceramic materials, which would improve the technological performance of glazes commonly used in the floor and wall tile manufacturing industry. The objectives of this study were as follows:

1) To develop and characterise glazes of a glass-ceramic nature, producing crystallisations within the glass matrix, by using previously selected frits, with the addition of nucleating agents in the formulation. These were then heat-treated in an industrial kiln used for glazed floor tile manufacture. Development was carried out for both red- and white-firing bodies.

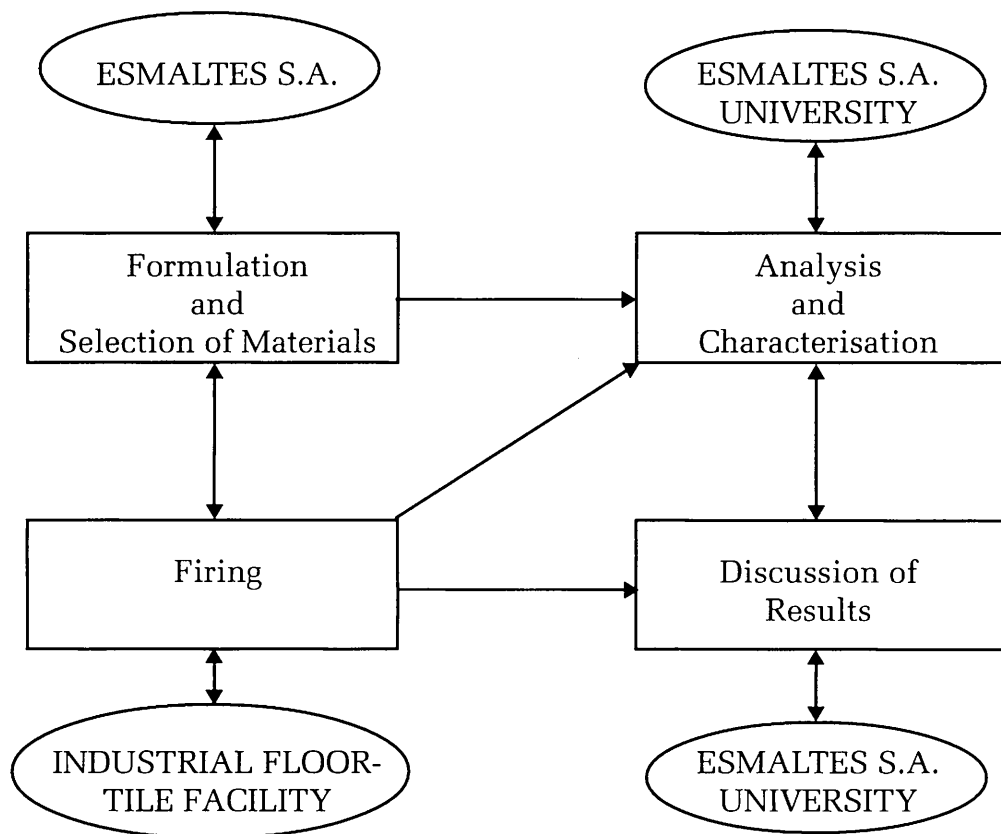
2) To obtain glass-ceramic composites from these glazes, of a high toughness by means of an α - Al_2O_3 , corundum addition with certain preset characteristics.

3) The final objective of the work was to achieve decoration of the body by screen-printing and granulates, which would maintain the mechanical properties achieved in the base glaze.

2. MATERIALS AND METHODS

2.1. METODOLOGY UDED

The methodology used in the development of this study is reflected in the following flow chart:



Flow Chart. Working Methodology

After choosing the raw materials, the glazes were formulated. These were wet ground in a fast alumina ball mill, at an oversize of 4 on a < 45 µm screen mesh and they were applied with an applicator to the previously engobed body. On single-firing in an industrial floor tile facility according to the corresponding cycle for the white or red body, the resulting fired tiles were analyzed and characterised. Following discussion of the results obtained in each phase or stage, new glazes were formulated, thus closing the cycle.

2.2. CHARACTERISATION TECHNIQUES

The following instrumental techniques were used to characterise the resulting materials:

- X-Ray Diffraction (XRD). Siemens D-5000 instrument, using $\text{CuK}\alpha$ radiation and a nickel filter and an automatic system for data acquisition and processing, which includes the JCPDS files. Tests were carried out by measuring between 2° and 70° , and between 10° and 65° , in the range 2σ , with a time constant of 1 s and a goniometer velocity of $0.02^\circ/2\theta$.
- Scanning Electron Microscope (SEM) and EDX microanalysis, using the following two instruments:
JEOL JSM 6300 and Link spectrometer, Oxford ISIS system.
HITACHI Series H-200 and KeveX spectrometer, Quantum-2000.
- UV-visible spectroscopy, with a Perkin-Elmer spectrophotometer, Model UV/VIS/NIR Lambda 19, with the solid diffuse reflectance method, incorporating CIE-Lab standard colour analysis. For measurement of the whiteness index, the apparatus was calibrated with high-purity magnesium oxide.
- Particle-size distribution, with an apparatus for determining particle sizes by laser diffraction, HELOS (Helium Neon Laser Optical Diffraction-Spectrometer for Particle Size Analysis) by SYMPATEC.
- Vickers microhardness tester, Model Matsuzawa MHT-1, of 2 kg maximum force.
- Mohs hardness measurements.
- Decorating techniques: screen-printing and granulate application
- Industrial firing kilns.

White body.- 82 m kiln with a peak temperature of 1170°C and a firing cycle of 52 minutes.

Red body.- 95 m kiln with a peak temperature of 1150°C and a firing cycle of 42 minutes.

3. EXPERIMENTAL DEVELOPMENT

For the sake of a greater understanding of the work carried out, the glazes used are referred to as PR and PB, for the red body and white body respectively.

3.1. SELECTION OF THE STARTING GLAZE COMPOSITION

The starting point was situated within the primary field of zircon in the phase diagram $\text{SiO}_2\text{-Al}_2\text{O}_3\text{-ZrO}_2$, where the possibility of crystal formation is greater (Fig. 5).

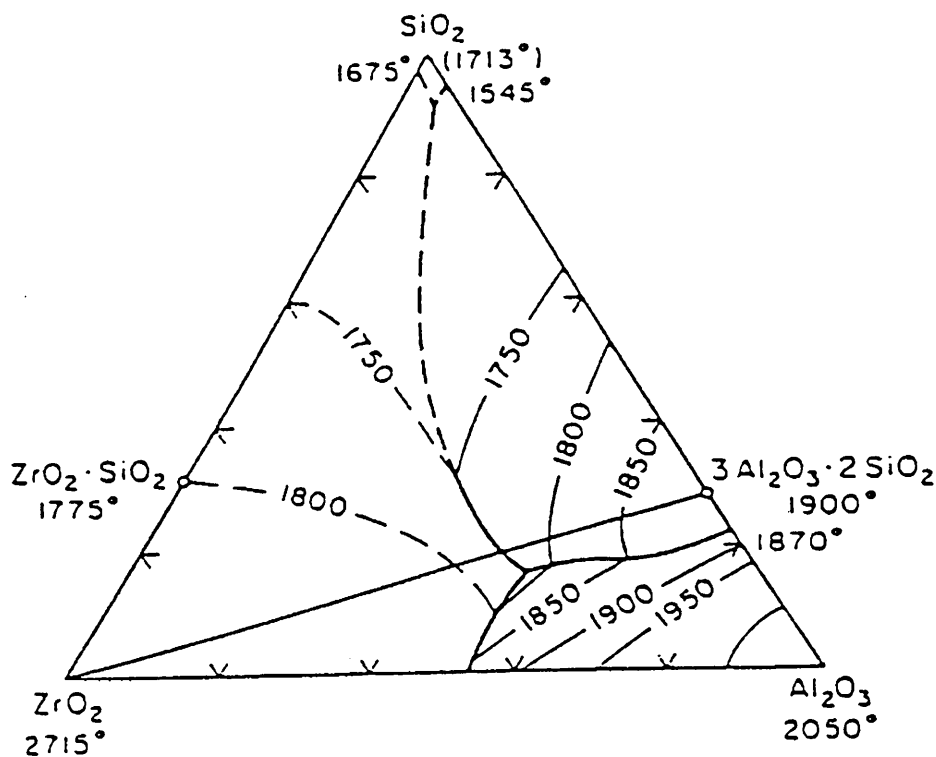


Figure 5. Phase diagram of the $\text{SiO}_2\text{-Al}_2\text{O}_3\text{-ZrO}_2$ system.

The qualitative composition of the starting glaze used, once the pre-selection study had been carried out, is shown in Table II.

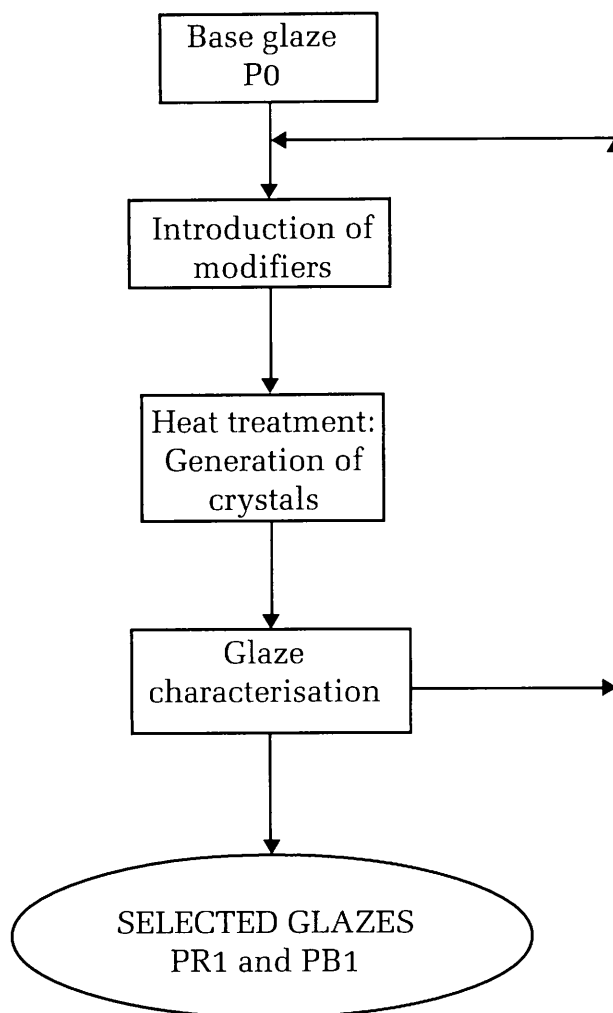
Table II. Qualitative composition of the starting glaze (P0)

OXIDE	Al_2O_3	SiO_2	ZrO_2	Other oxides
% by weight	0 - 20	50 - 60	7 - 12	<5

3.2. STUDY OF THE DEVITRIFICATION PROCESS.

Using the base or starting glaze, whose qualitative composition is shown in Table II, different compositions were tested in order to generate a greater number of ZrSiO_4 crystallisations within the glassy phase by means of devitrification processes, keeping the industrial firing cycle constant.

Testing consisted of varying the main components and introducing devitrifying agents, which affected the viscosity of the starting glaze in firing.



Flow chart 2. Methodology for experimental development.

3.3. STUDY OF NUCLEATING AGENTS

The nucleation of glass begins when there exists an ordered molecular grouping of the glass components, which give rise to crystalline seeds.

In order to generate a greater number of zircon crystallisations in the glazes developed and selected in the previous section (PR1 and PB1), a study was carried out on the introduction of nucleating agents of different chemical nature.

For the two types of body, the effect was studied of the addition to the composition of five nucleating agents (Table III), of which two were light element oxides (A and B), and three were heavier elements (C, D and E).

The addition of the nucleant was carried out by adding the percentage by weight of the nucleating agent to the glaze formula.

Table III. Weight percentage of the added nucleating agent.

REFERENCE	%NUCLEANT
AR1, BR1, CR1, DR1, ER1, AB1, BB1, CB1, DB1, EB1	0.5
AR2, BR2, CR2, DR2, ER2 AB2, BB2, CB2, DB2, EB2	1.0
CR3, DR3, ER3 CB3, DB3, EB3	2.0

where A, B, C, D and E are different nucleating agents; R and B correspond to the glaze developed on a red or white body respectively; and 1, 2 and 3 are the percentages of the added nucleant.

3.4. FORMATION OF COMPOSITES

The possibility was considered of improving even more the mechanical properties of the glaze obtained by means of the formation of super-tough composites within the devitrified material, on the basis of the improved results obtained in the formulations shown in Table III. The methodology used was the introduction of α -alumina without exceeding 10% by the weight as indicated in the introduction, based on the literature surveyed.

4. RESULTS AND DISCUSSION

4.1. STARTING GLAZE

Firstly, the glaze previously selected as the starting glaze was characterised (Table III). For this purpose X-ray diffraction analysis was used (henceforth referred to as XRD) of the powdered glaze before firing (Fig. 6) in which the presence of crystallographic phases of baddeleyite, ZrO_2 ⁽¹⁾, quartz SiO_2 ⁽³⁾, and corundum $\alpha-Al_2O_3$ ⁽⁴⁾ was observed, where the major crystalline phase was baddeleyite, which exhibited a low degree of crystal development, given the number of counts obtained.

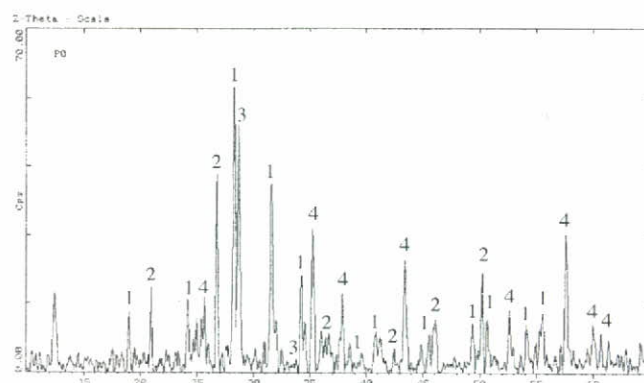


Figure 6. XRD analysis of the starting glaze (P0) before application and heat treatment in the industrial kiln.

- (1) ZrO_2 baddeleyite, ASTM File No. 4-1165.
 (2) SiO_2 quartz, ASTM File No. 33-1161
 (3) SiO_2 coesite, ASTM File No. 14-0654
 (4) $\alpha-Al_2O_3$ corundum, ASTM File No. 42-1468

The results obtained from the glaze applied on red-bodied tiles (PR0) and white-bodied tiles (PB0) are summarised in Table IV:

Table IV: Values obtained from the analysis performed in the starting glaze.

Reference	XRD ⁽¹⁾ (no. of counts)	Vickers Microhardness, Hv (kgf/mm ²)	Mohs Hardness	Whiteness Index ⁽²⁾
PR0	97	458	4	11.723
PB0	69	510	6	12.906

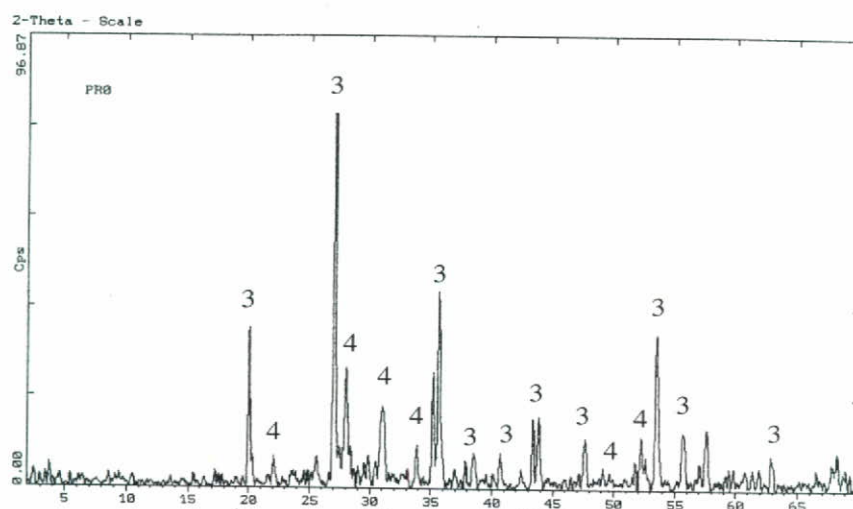
(1) Number of counts of the maximum intensity peak of the diffractogram corresponding to the zircon crystalline phase.

(2) Whiteness index measured on a MgO standard of $I_b = 8.3318$ (ASTM 1925)

The analytical results obtained by XRD show the presence of $ZrSiO_4$ as the major phase and also small anorthitic-type crystallisations $CaAl_2Si_2O_8$,⁽⁴⁾ in the glaze applied on the redware tile, whereas in the same glaze on the whiteware tile, zircon $ZrSiO_4$ appeared as the major crystalline phase with small crystallisations of corundum $\alpha-Al_2O_3$ ⁽⁵⁾ and spinel $MgAl_2O_4$ ⁽⁶⁾.

The crystalline phases arising during firing were zircon, anorthite and spinel. The rest were introduced as raw materials in the glaze formulation. It should be pointed out that the degree of crystallisation which appears is very low.

Fig. 7 shows the diffractograms corresponding to the fired glazes.



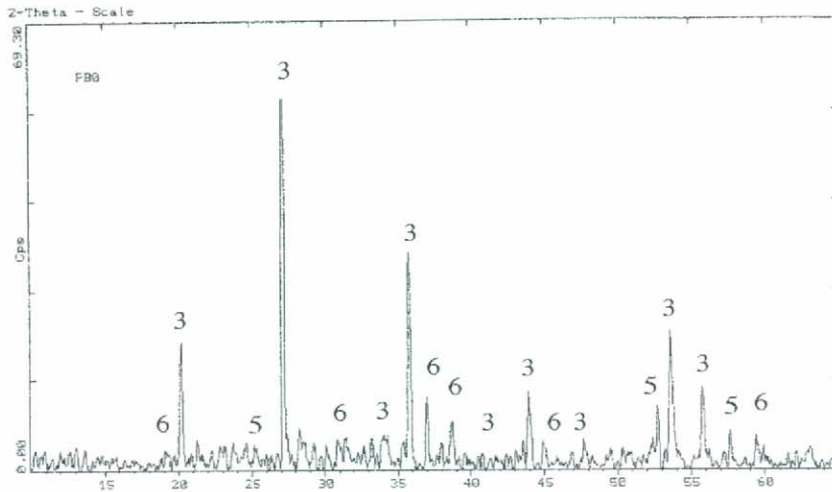


Figure 7. XRD of fired starting glaze PR0 (red body) and PB0 (white body).

- | | |
|----------------------|-----------------------------------|
| (3) $ZrSiO_4$ | zircon, ASTM File No. 6-0266. |
| (4) $CaAl_2Si_2O_8$ | anorthite, ASTM File No. 20-0020. |
| (5) $\alpha-Al_2O_3$ | corundum, ASTM File No. 42-1468 |
| (6) $MgAl_2O_4$ | spinel, ASTM File No. 21-1152. |

It should also be noted that although the arising zirconium silicate recorded by the diffractogram was greater in the glaze on the red body, which yielded enhanced whiteness of the material, lower mechanical strength values were found than those of the glaze on the white body. This was possibly caused by the firing cycle, since it varied in both types of body; the temperature reached in the red body being lower.

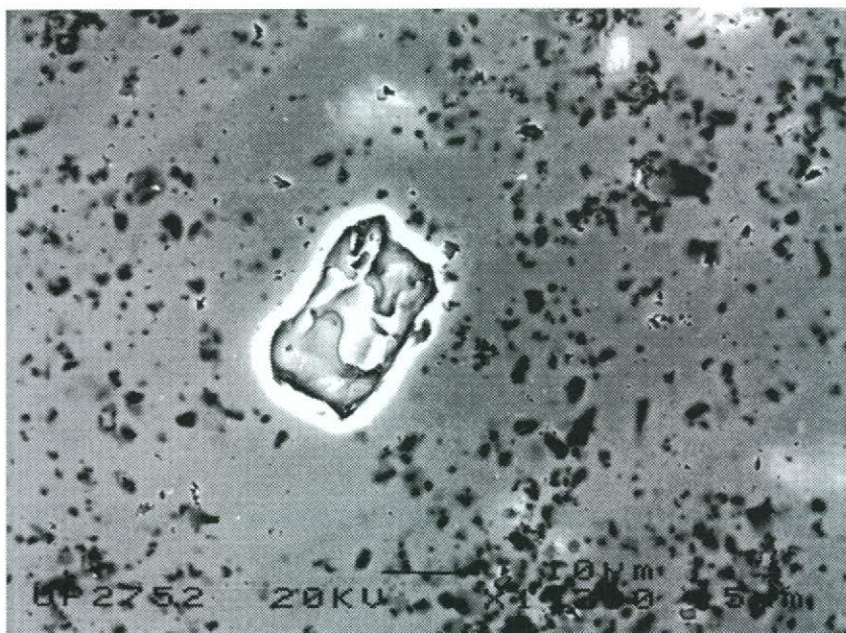


Figure 8 a) SEM micrograph of the starting glaze (PR0).

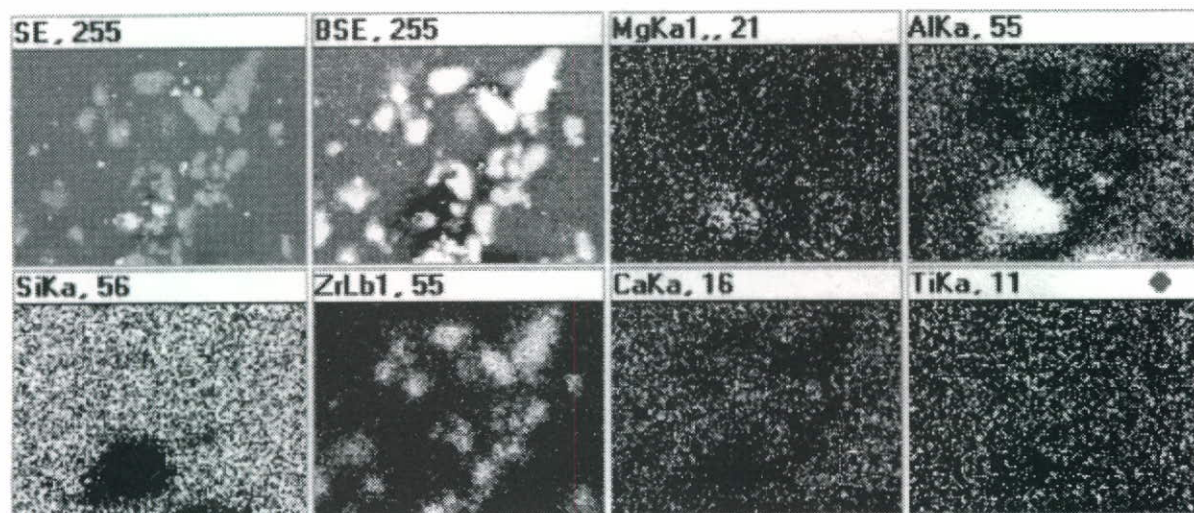


Figure 8 b) EDX surface mapping

Fig. 8 a) shows small crystals ($< 1 \mu\text{m}$) on an amorphous matrix, and the surface mapping (or surface element distribution analysis) shows the presence of areas of aluminium, silicone and zirconium concentrations, as being the most important elements. The presence of crystallisations which may be seen both in the image obtained using secondary electrons ("SE" in the micrograph on the left), and in the image obtained using back-scattered electrons ("BSE" in the micrograph on the right), where more are detected, while the heaviest elements show up brightest. Both the zirconium and the silicon appear concentrated in the micrograph, which shows the formation of crystals which may be assigned to the zircon ZrSiO_4 , as confirmed by XRD. It should be noted that in these points no concentration of the other elements appear.

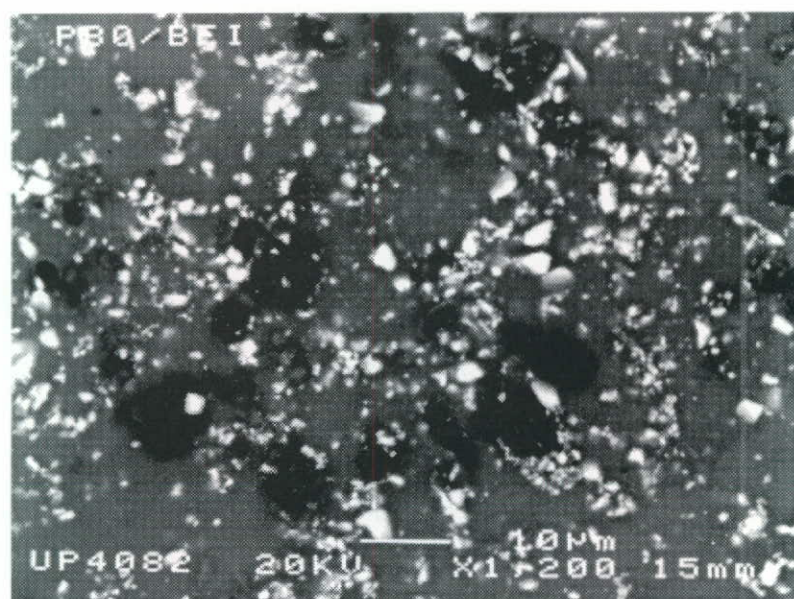


Figure 9 a) SEM micrograph of the starting glaze (PB0).

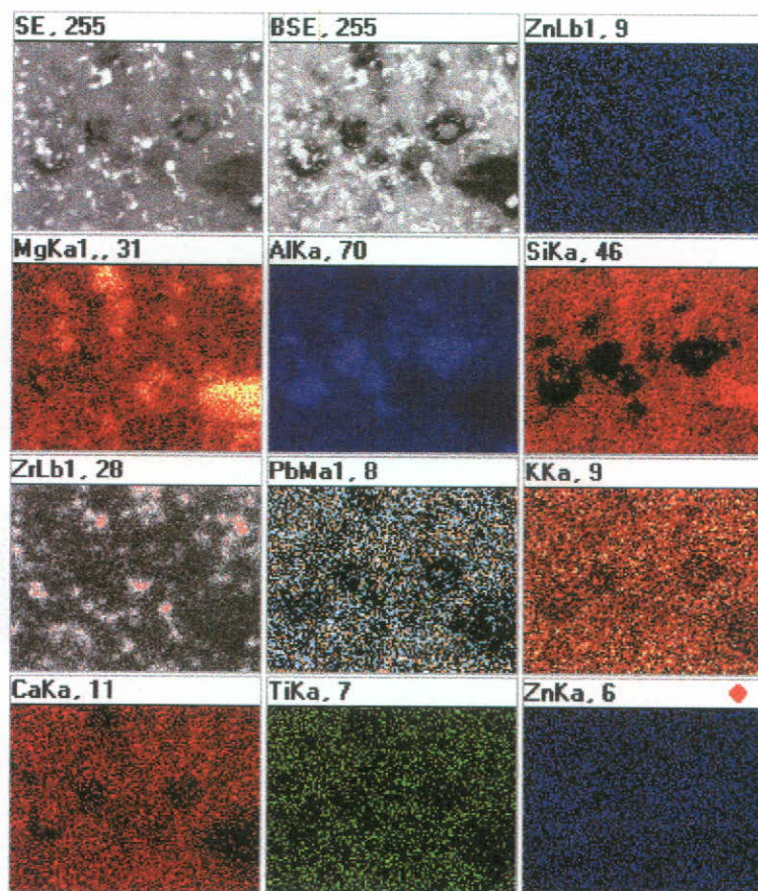


Figure 9 b) Surface mapping using EDX

In the micrograph (Fig. 9 a), there appear crystallisations of a similar size and number to the corresponding ones in the red body (PR0). The mapping is shown in Fig. 9 b which also shows concentrations of zirconium and silicon on the brightest crystals, in accordance with the XRD results where zircon $ZrSiO_4$ appears. There also appear concentrations of magnesium, which, as can be seen in the XRD, forms part of spinel $MgAl_2O_4$ crystals. Points may also be seen where there is a concentration of aluminium, and which may be identified as crystals of corundum, α -alumina in the XRD.

4.2. RESULTS OBTAINED IN THE DEVITRIFICATION PROCESS

Given the results, an attempt was made to increase the mechanical strength of the material by trying to produce devitrifications in the glaze and increase the number of zircon $ZrSiO_4$ crystallisations.

In the XRD analysis of the unfired glazes, both in the glaze developed for the red body and that for the white body (Fig. 10), the same crystalline phases may be observed as in the starting glaze (P0).

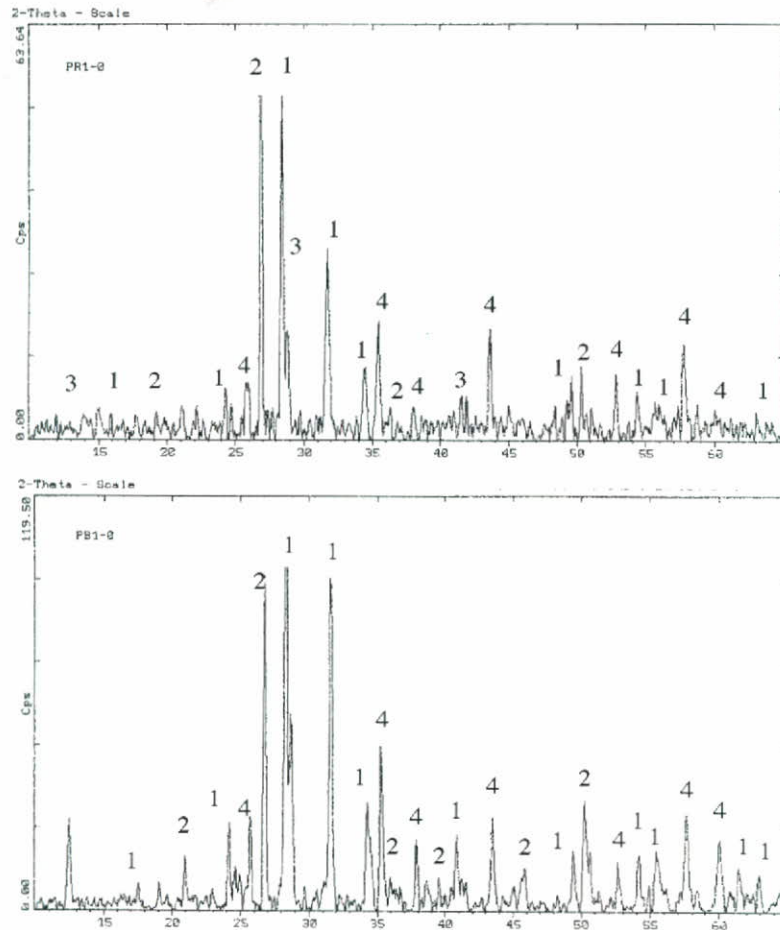


Figure 10. XRD analysis of the unfired glazes (PR1-0, red body; PB1-0, white body).

- (1) ZrO_2 baddeleyite, ASTM File No. 24-1165.
- (2) SiO_2 quartz, ASTM File No. 33-1161'
- (3) SiO_2 coesite, ASTM File No. 14-0654'
- (4) $\alpha-Al_2O_3$ corundum, ASTM File No. 42-1468

The analytical data obtained with the new glazes developed after heat treating the ceramic body (PR1, glaze for red body; PB1, glaze for white body) are shown in Table V.

Table V. Values obtained from the analyses performed on PR1 and PB1.

Reference	XRD ⁽¹⁾ (no. of counts)	Vickers Microhardness, Hv (kgf/mm ²)	Mohs Hardness	Whiteness Index ⁽²⁾
PR1	141	515	6	10.311
PB1	118	528	7	12.119

(1) Number of counts of maximum intensity peaks of the diffractogram, corresponding to the zircon crystalline phase.'

(2) Whiteness index measured on a MgO standard of $I_b = 8.3318$ (ASTM 1925).

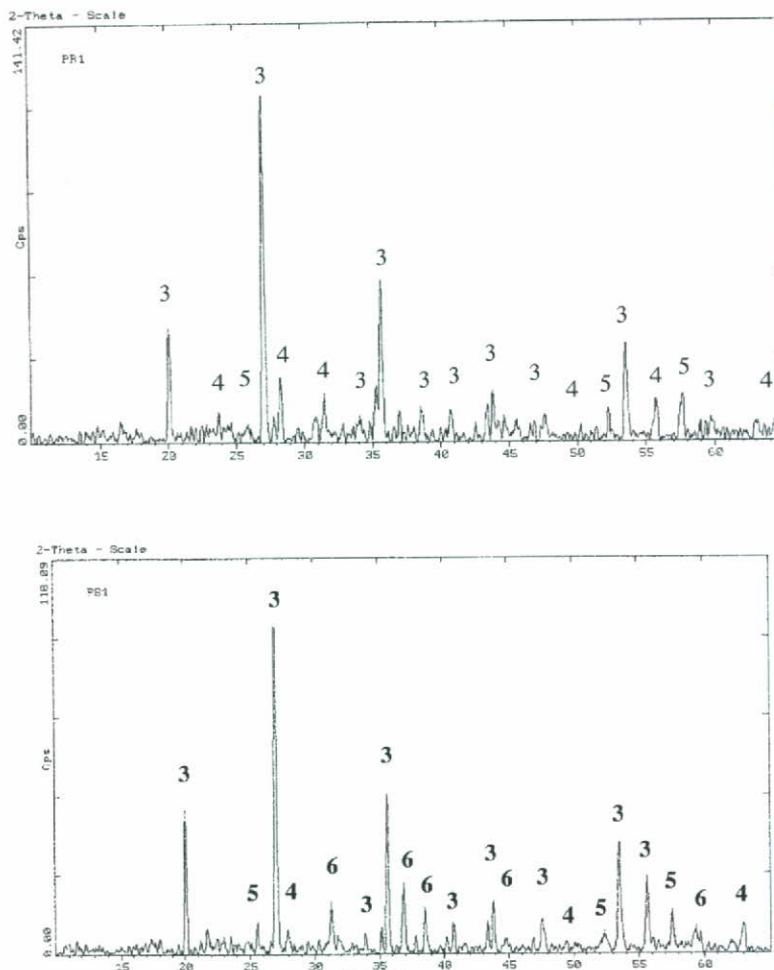


Figure 11. XRD diffractograms of fired glazes PR1 (red body) and PB1 (white body).

- | | |
|----------------------|-------------------------------------|
| (3) $ZrSiO_4$ | zircon, ASTM File No. 6-0266. |
| (4) ZrO_2 | baddeleyite, ASTM File No. 24-1165. |
| (5) $\alpha-Al_2O_3$ | corundum, ASTM File No. 42-1468 |
| (6) $MgAl_2O_4$ | spinel, ASTM File No. 21-1152. |

On comparison of the XRD analyses of the unfired glazes with the fired ones we can see that the most intense peaks, corresponding to the baddeleyite crystalline phase, which appear in the unfired glaze diffractograms, almost disappear in the diffractograms of the fired glazes, with zircon developing after heat treatment.

In both types of body, the major crystallisations are those of zircon $ZrSiO_4$, although the number of counts, and therefore the degree of crystallinity is still greater in the case of the glaze applied to the red body. It is important to note the increase in the Vickers microhardness and Mohs hardness values. A greater degree of whiteness may also be observed, linked to the increased crystallisation.

The results of the microstructural and microanalytical study are shown in Figs. 12 and 13.

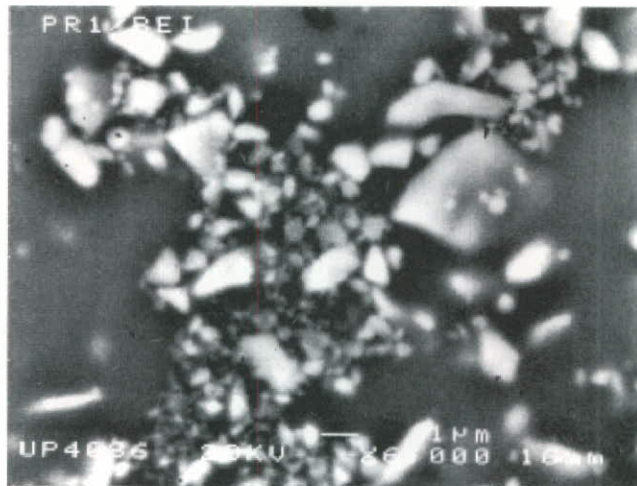


Figure 12-a) SEM micrographs using BSE of the glaze for the red body (PR1).

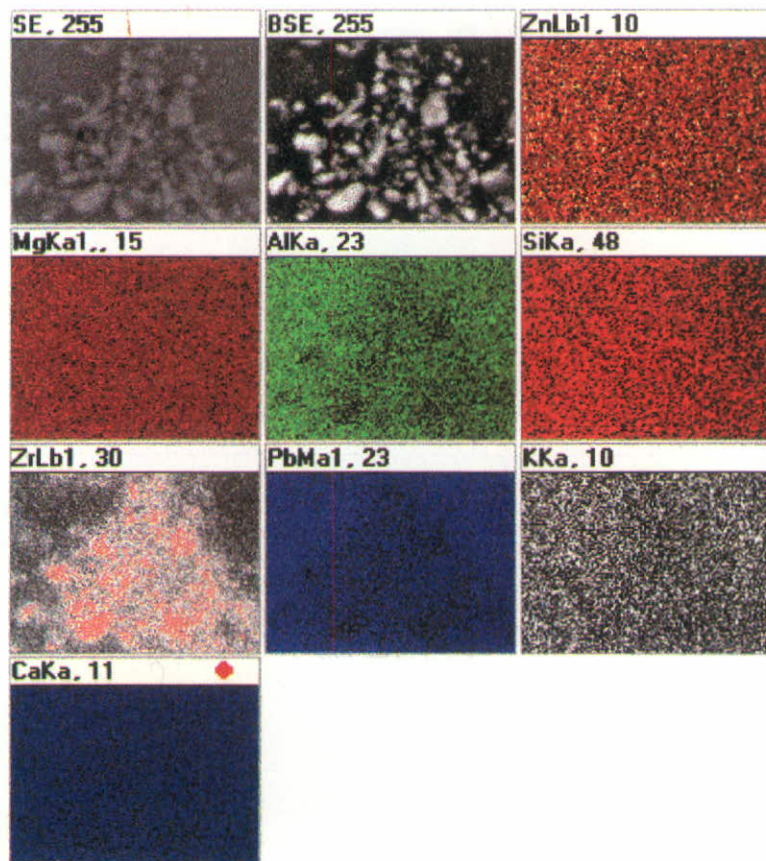


Figure 12-b) Surface mapping, using EDX.

The micrograph shows a large number of bright crystals with sizes which vary between 1 and three μm . EDX microanalysis of these crystals shows a constant Si-Zr ratio, which is also consistent with XRD outcomes, which indicate the formation of zircon ZrSiO_4 . In the mapping analysis (Fig. 12-b) the concentration of zirconium in these crystals may also be seen, thus matching the XRD data and highlighting the great number of these crystals.

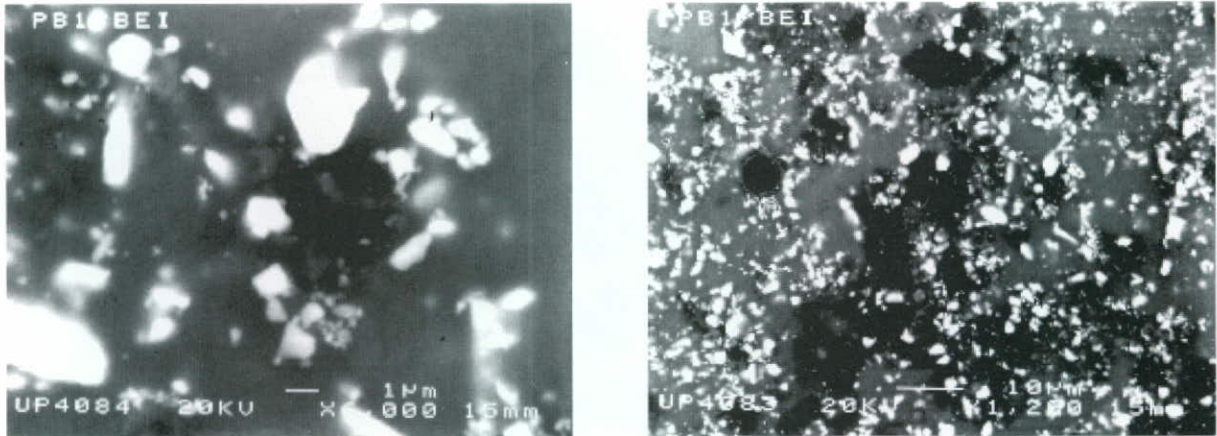


Figure 13-a) SEM micrograph using BSE of the glaze for the white body (PB1).

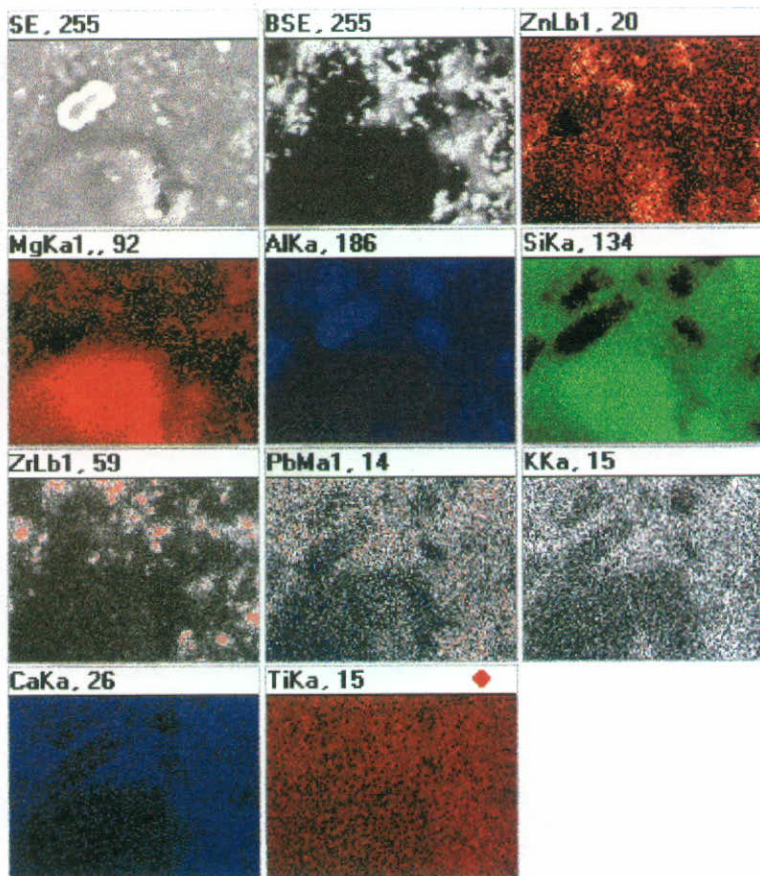


Figure 13-b) Surface mapping, using EDX.

In the microstructural and microanalytical study of the PB1 test specimen, brighter crystals of a greater zirconium concentration may be observed, which could correspond to the zircon crystalline phases detected in the XRD. The number of these crystals in the observation field is slightly smaller than in the case of the PR1 sample. There also appear darker areas in the BSE micrograph, where the aluminium is seen to be concentrated. This would correspond to crystals of α -alumina, corundum, detected by XRD. In the mapping

analysis there also appear concentrated areas of magnesium, which would correspond to the crystallisations of spinel $MgAl_2O_4$, detected by XRD.

4.3. RESULTS OBTAINED WITH THE INTRODUCTION OF NUCLEATING AGENTS.

The diffractograms of the unfired glazes into which nucleating agents were introduced (Table III), show the same crystalline phases as the diffractograms of unfired glazes in the previous stage, as well as the peaks corresponding to the added nucleating agents.

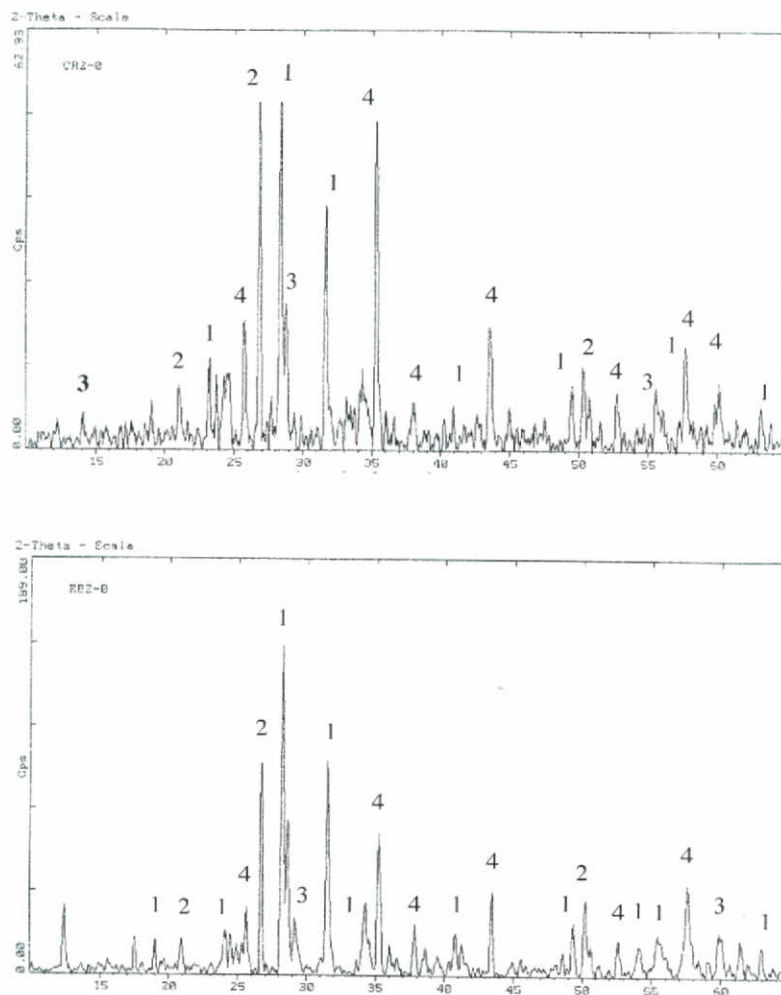


Figure 14. XRD analysis of glazes CR2-0 (red body) and EB2-0 (white body).

- (1) ZrO_2 baddeleyite, ASTM File No. 24-1165.
- (2) SiO_2 quartz, ASTM File No. 33-1161
- (3) SiO_2 coesite, ASTM File No. 14-0654
- (4) $\alpha-Al_2O_3$ corundum, ASTM File No. 42-1468

The results obtained in the glazes developed on the red body after industrial firing, with the selected nucleating agents listed in Table III are shown in the following table:

Table VI. Influence of nucleating agents (Red Body).

Reference	XRD ⁽¹⁾ (no. of counts)	Vickers Microhardness, Hv (kgf/mm ²)	Mohs Hardness	Whiteness Index ⁽²⁾
AR1	240	580	6	9.466
AR2	311	609	6	8.884
BR1	211	573	6	11.174
BR2	214	536	6	10.603
CR1	236	614	8	9.510
CR2	248	621	8	9.612
CR3	362	540	7	9.844
DR1 ⁽³⁾	—	—	-	-
DR2 ⁽³⁾	—	—	-	-
DR3 ⁽³⁾	—	—	-	-
ER1	158	604	7	9.333
ER2	167	506	7	9.173
ER3	144	529	7	9.558

(1) Number of counts of the maximum intensity peak of the diffractogram corresponding to the zircon crystalline phase.

(2) Whiteness index measured on a MgO standard of $I_b = 8.3318$ (ASTM 1925).

(3) Not characterised due to the existence of faults in the tiles.

On the basis of the figures given in Table VI the role played by the nucleating agent may be observed. The “C” nucleant is the most effective as it yields the best properties.

In all the diffractograms (Fig. 15) zircon $ZrSiO_4$ ⁽¹⁾ appears as the major crystalline phase. Small crystallisations of corundum $\alpha-Al_2O_3$ ⁽²⁾ appear together.

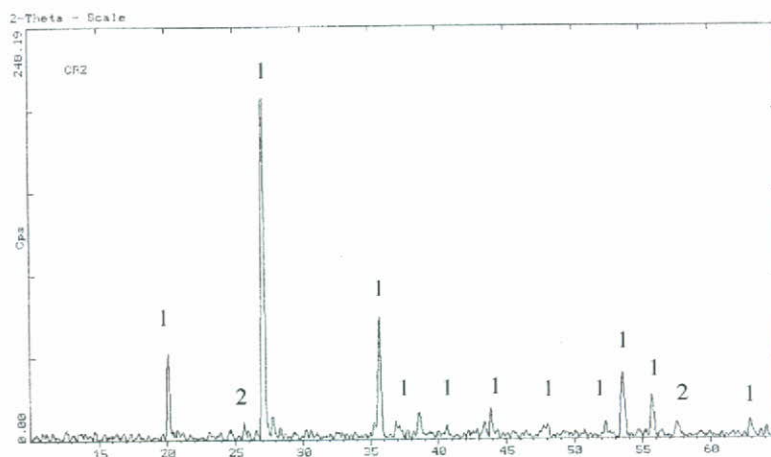


Figure 15. XRD analysis of the CR2 test specimen (red body).

(1) $ZrSiO_4$ zircon, ASTM File No. 6-0266.

(2) $\alpha-Al_2O_3$ corundum, ASTM File No. 42-1468

The results obtained in the glazes developed on the white body with the selected nucleating agents listed in Table III are summarised in Table VII.

Table VII. Influence of nucleating agents (White Body)

Reference	XRD ⁽¹⁾ (no. of counts)	Vickers Microhardness, Hv (kgf/mm ²)	Mohs Hardness	Whiteness Index ⁽²⁾
AB1	246	527	6	12.295
AB2	127	564	6	12.378
BB1	90	540	7	12.228
CB1	249	591	6	10.632
CB2	248	581	8	11.357
CB3	337	581	8	11.752
DB1 ⁽³⁾	—	—	-	-
DB2 ⁽³⁾	—	—	-	-
DB3 ⁽³⁾	—	—	-	-
EB1	223	669	8	11.592
EB2	224	734	8	11.265
EB3	226	671	8	12.348

⁽¹⁾ Number of counts of the maximum intensity peak of the diffractogram corresponding to the zircon crystalline phase.

⁽²⁾ Whiteness index measured on a MgO standard of $I_b = 8.3318$ (ASTM 1925).

⁽³⁾ Not characterised due to the existence of faults in the tiles.

On the basis of the figures given in Table VII, it may be seen that the best results were obtained using nucleant "E".

XRD analysis (Fig. 16.) also shows that the major crystalline phase in the diffractograms of the fired glazes is zircon $ZrSiO_4$ ⁽¹⁾ with small crystallisations of corundum $\alpha-Al_2O_3$ ⁽²⁾ and spinel $MgAl_2O_4$ ⁽³⁾.

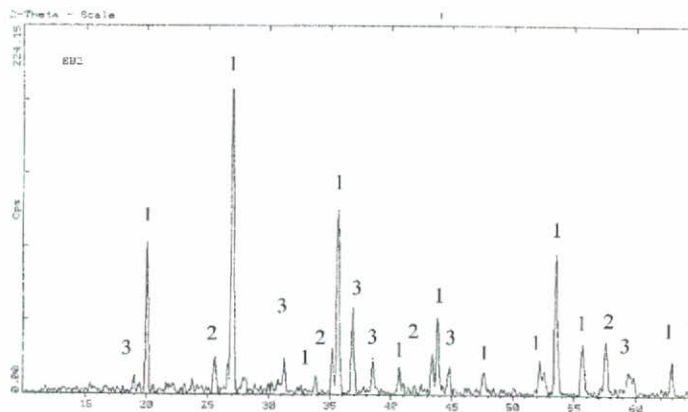


Figure 16. XRD analysis of the EB2 test specimen (white body).

⁽¹⁾ $ZrSiO_4$ zircon, ASTM File No. 6-0266.

⁽²⁾ $\alpha-Al_2O_3$ corundum, ASTM File No. 42-1468

⁽³⁾ $MgAl_2O_4$ spinel, ASTM File No. 21-1152.

4.4. FORMATION OF COMPOSITES

XRD analyses of unfired glazes with an addition of $\alpha\text{-Al}_2\text{O}_3$ (Fig. 17) show the same crystalline phases as the diffractograms of the test specimens in the previous section, with a considerable increase in the degree of crystallinity of the $\alpha\text{-Al}_2\text{O}_3$ phase.

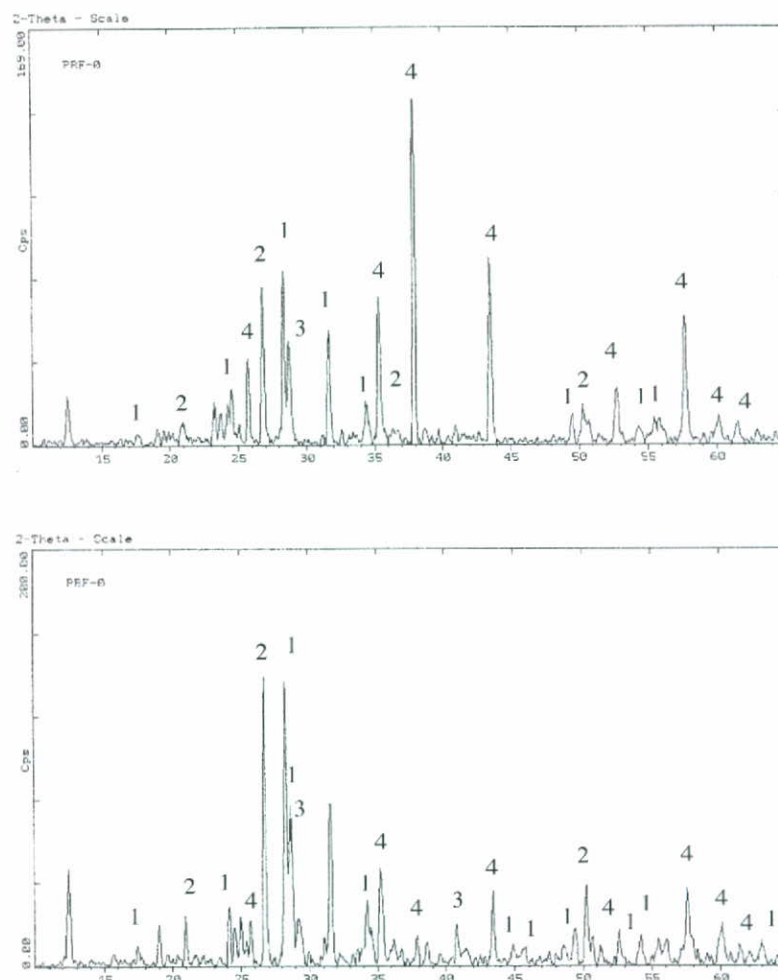


Figure 17. XRD analysis of test specimens PRF-0 (red body) and PBF-0 (white body) before heat treatment.

- (1) ZrO_2 baddeleyite, ASTM File No. 24-1165.
- (2) SiO_2 quartz, ASTM File No. 33-1161
- (3) SiO_2 coesite, ASTM File No. 14-0654
- (4) $\alpha\text{-Al}_2\text{O}_3$ corundum, ASTM File No. 42-1468

In the tests performed on both red and white bodies after heat treatment, an increase in the degree of crystallinity was observed, which caused a considerable improvement in the mechanical properties. The crystalline phases shown in XRD analysis (Fig. 18) were zircon ZrSiO_4 ⁽¹⁾ as the major phase and corundum $\alpha\text{-Al}_2\text{O}_3$ ⁽²⁾, with spinel MgAl_2O_4 ⁽³⁾ appearing as a third crystalline phase in the tests performed on the white body.

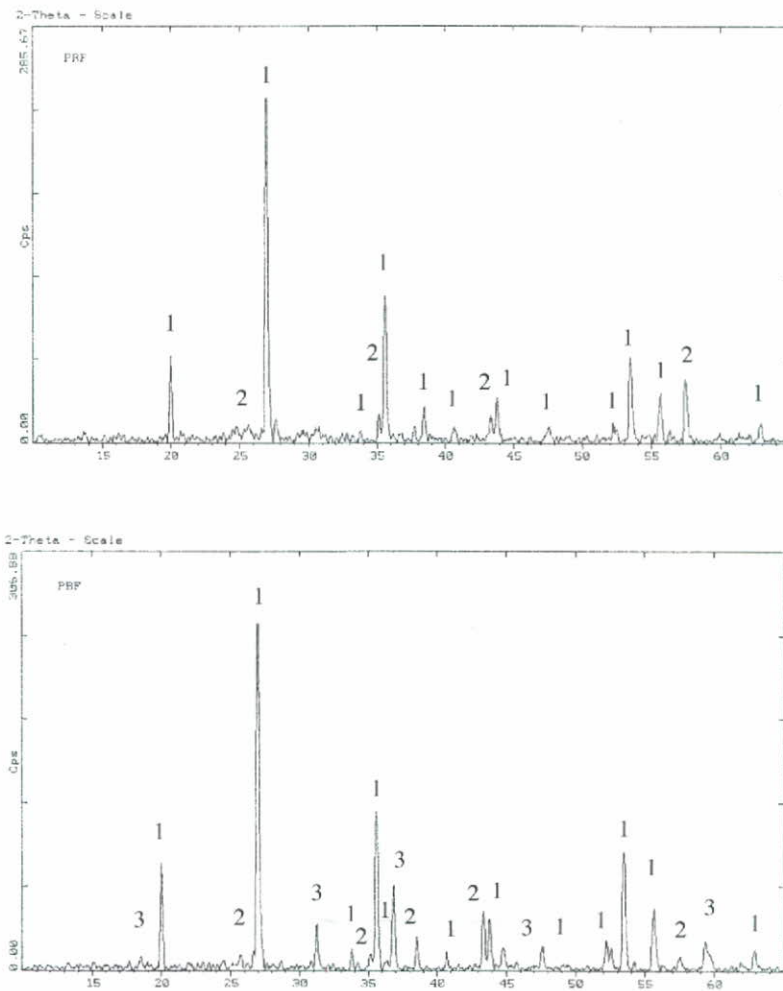


Figure 18: XRD analysis of test specimens PRF (red body) and PBF (white body).

- (1) $ZrSiO_4$ zircon, ASTM File No. 6-0266.
- (2) $\alpha-Al_2O_3$ corundum, ASTM File No. 42-1468
- (3) $MgAl_2O_4$ spinel, ASTM File No. 21-1152.

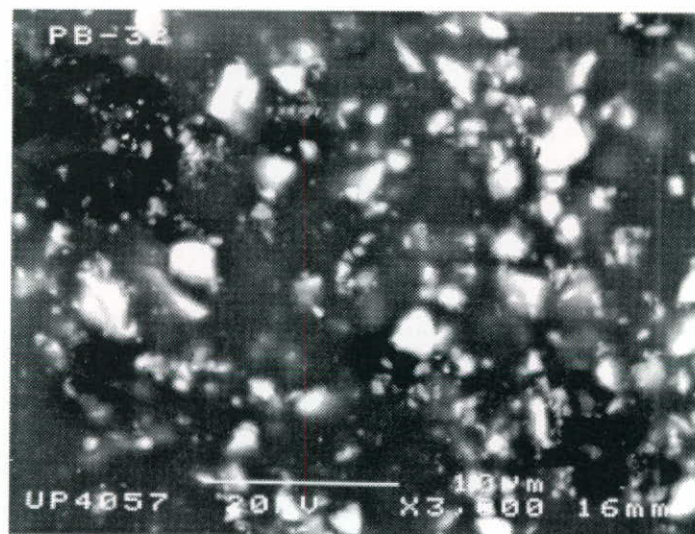


Figure 19-a) SEM micrograph of test specimen PBF (White body).

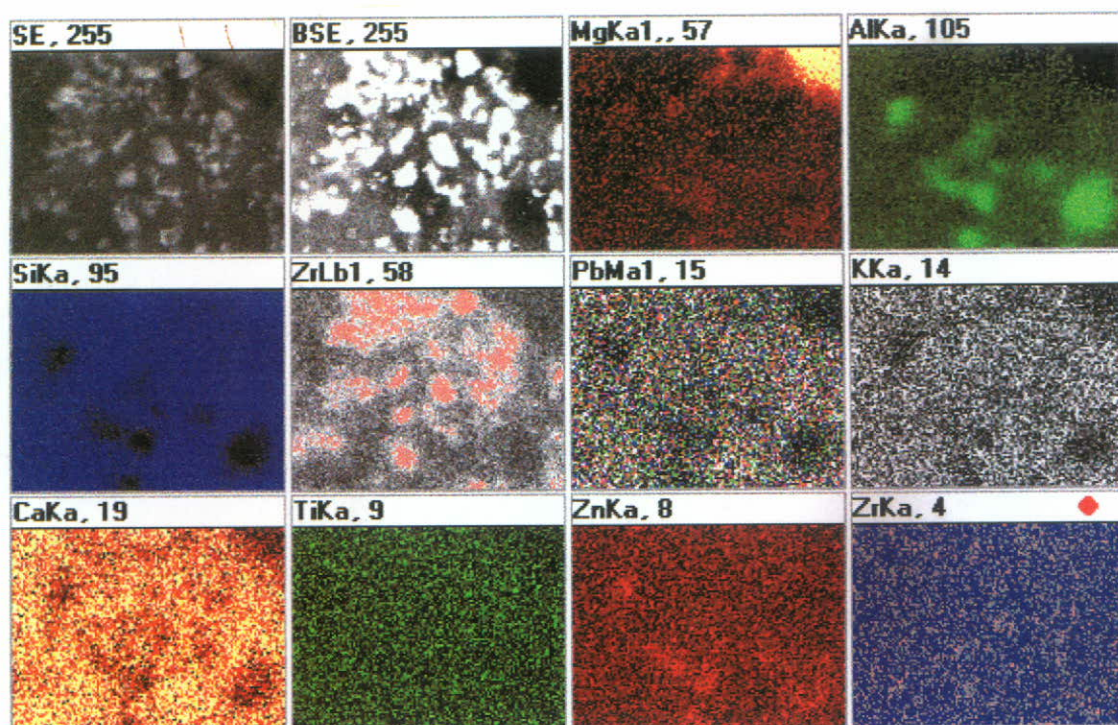


Figure 19-b) EDX microanalysis of test specimen PBF (White body).

The morphological and microanalytical analysis shows the presence of bright crystals, using the BSE observation technique. Analysis of these shows a constant Si-Zr ratio, as well as a high concentration of zirconium when mapping is performed. These are large in size and great in number. Darker areas also appear in the micrograph, analysis of which indicates a high concentration of aluminium, as can be observed in the mapping analysis. This agrees with the presence of $\alpha\text{-Al}_2\text{O}_3$ introduced as corundum and analyzed using XRD.

Similar results were obtained for the glaze on the red body.

The results obtained after firing these test specimens are shown in Table VIII.

Table VIII. Values obtained after formation of the alumina composites.

Reference	XRD ⁽¹⁾ (no. of counts)	Vickers Microhardness, Hv (kgf/mm ²)	Mohs Hardness	Whiteness Index ⁽²⁾
PRF	286	691	9	9.716
PBF	307	784	9	11.493

⁽¹⁾ Number of counts of the maximum intensity peak of the diffractogram corresponding to the zircon crystalline phase.

⁽²⁾ Whiteness index measured on a MgO standard of $I_b = 8.3318$ (ASTM 1925).

5. APPLICATION OF THE PRODUCTS OBTAINED IN CERAMIC DESIGN.

For screen-printing decoration, the development of a crystalline-type frit with a hardness similar to that of the starting glaze was set as an objective, in order not to lose in decoration the improved mechanical properties that had been obtained in the starting glaze. It was thus decided to attempt to develop a frit with a tendency to anorthitic devitrification ($\text{CaAl}_2\text{Si}_2\text{O}_8$).

In order to develop this frit, an exhaustive study was carried out of the quaternary phase diagram: SiO_2 - Al_2O_3 - CaO - MgO (Fig. 20), from which a composition was chosen within the anorthite primary field, as close as possible to that of cordierite, though always within the logical constraint stemming from the temperature cycles used in industrial frit kilns (maximum temperature of 1500°C).

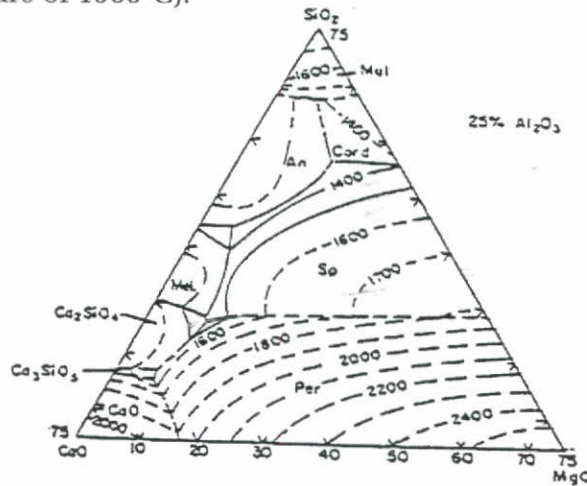


Figure 20. Phase diagram SiO_2 - Al_2O_3 - CaO - MgO

Table IX shows the qualitative composition of the frit to be developed.

Table IX. Qualitative composition of the formulated frit.

OXIDE	Al_2O_3	CaO	MgO	SiO_2
% by weight	10-40	10-40	10-40	40-60

In the frit applied as a glaze to a ceramic body, and after heat treatment performed in the industrial kiln, SEM/EDX microscopy (Fig. 21) showed the presence of a large quantity of anorthitic-type $\text{CaAl}_2\text{Si}_2\text{O}_8^{(1)}$ crystallisations, the XRD diffractogram for which is depicted in Fig. 22.

It has also been possible, after performing a morphological study using electron microscopy and energy dispersive microanalysis (SEM/EDX), to determine the presence of other crystals, which, once analyzed by means of specific analysis, demonstrated the existence of Ca, Si, Al and Mg (Fig. 23), indicative of the presence of crystallisations of a cordieritic nature (larger-sized crystals but few in number in each field of observation).

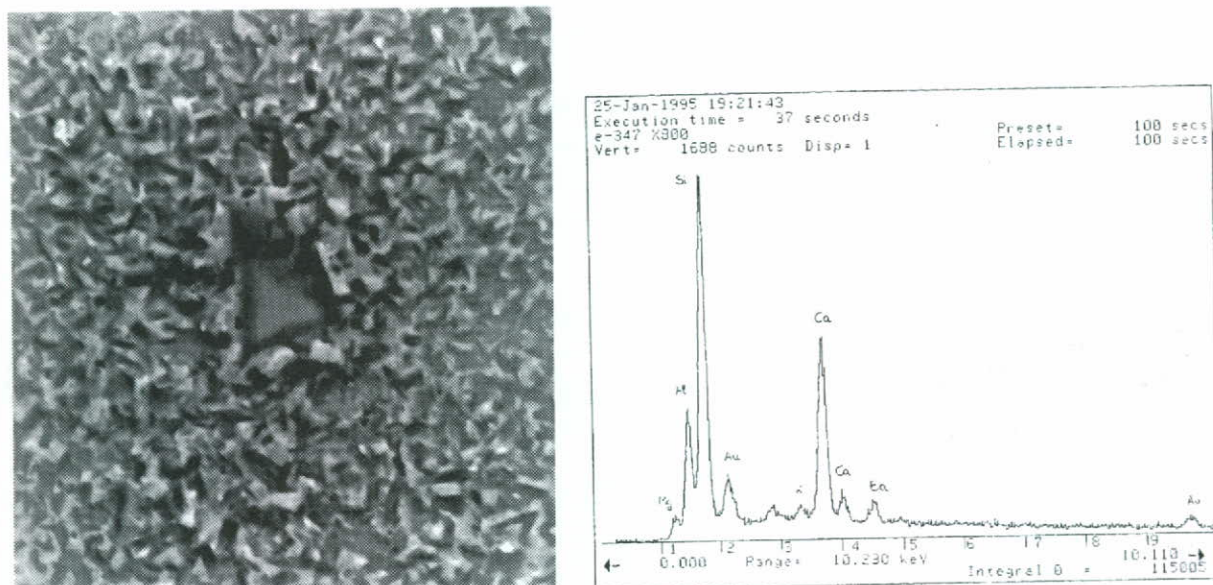


Figure 21.- SEM micrograph and EDX microanalysis of the frit used for screen-printing.

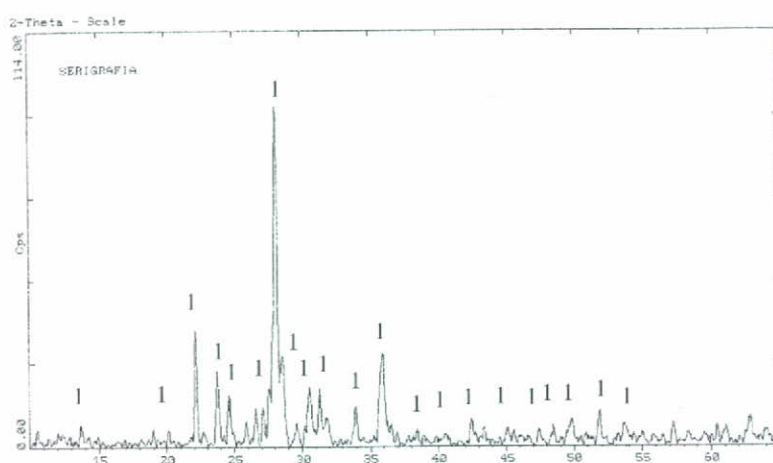


Figure 22.- XRD diffractogram of the frit used for screen-printing.

⁽¹⁾ $\text{CaAl}_2\text{Si}_2\text{O}_8$, anorthite, ASTM File No. 12-0301.

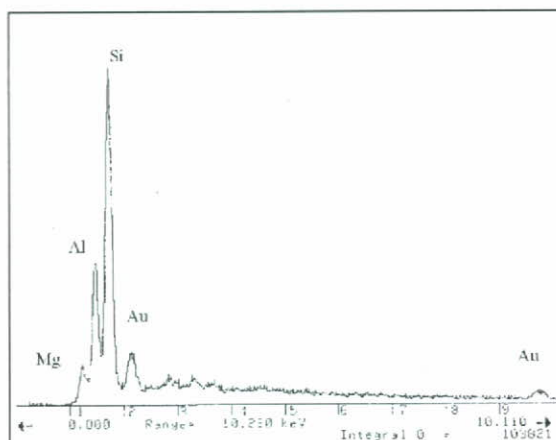


Figure 23. EDX microanalysis of a crystal of cordieritic composition.

The characteristics of the frit used for screen-printing decoration are shown in Table X.

Table X. Results of the analyses performed on the frit used for screen-printing, applied to a glazed tile.

XRD (no. of counts) ⁽¹⁾	Vickers Microhardness, (Hv kgf/mm ²)	Mohs Hardness
114	652	6 - 7

⁽¹⁾ Number of counts of the maximum intensity peak of the diffractogram corresponding to the anorthite crystalline phase.

For the granulate, a glaze was sought with technical characteristics as similar as possible to those of the starting glaze. This was then used to prepare an agglomerate, in the form of granules (pellets) with a size of between 606 and 454 μm .

6. CONCLUSIONS

- During the devitrification process, the level of crystallisation of zircon ZrSiO_4 was increased, thus attaining improvements in both the Vickers microhardness and Mohs hardness values.

- The degree of whiteness increases as a greater number of zircon crystallisations arise, as occurs in the first three steps.

- The addition of nucleating agents gives rise to an increase in the degree of crystallinity and better mechanical properties in the material. The best results were achieved with the "E" nucleant for the white body and the "C" nucleant for the red body.

- On adding the α -alumina to achieve the formation of composites, there was a slight decrease in the degree of whiteness of the fired glaze, but this drop was compensated for by a greater increase in mechanical properties.

- The glass-ceramic characteristics of all the components of the final product (base glaze, screen-print and granulate) have been shown, which make up an fully glass-ceramic product.

- The high technological performance of the glazes obtained justifies classifying them as high-toughness materials.

REFERENCES

1.- A. S. Jayatilaka, "Fracture of Engineering Brittle Materials", publ. Applied Science Publishers Ltd., London 1979."UKES"

2.- J. R. Jurado, "Propiedades de Materiales Cerámicos Avanzados: Propiedades Mecánicas". Conferences held during the Comett II Course: "Cerámicas Avanzadas, Materiales Vítreos y Vitrocerámicos", Department of Experimental Sciences of the Universitat Jaume I, September 1994. Published in Cerámica Información: Especial Curso Comett II" 209, 1995.

3.- "Nuevos Productos y Tecnologías de Esmaltes y Pigmentos Cerámicos", J. M. Rincón, J. Carda and J. Alarcón, publ. Faenza Editrice Ibérica y Sociedad Española de Cerámica y Vidrio, Castellón, 1992.

4.- J. M. Rincón, "Características especiales de los sistemas vítreos aplicables a la producción de nuevos esmaltes cerámicos", in "Nuevos Productos y Tecnologías de Esmaltes y Pigmentos Cerámicos", Ch. 1 pp. 13-38, publ. Faenza Editrice Ibérica y Sociedad Española de Cerámica y Vidrio, Castellón, 1992"ESUK"

5.- Seminar on the Environment, organized by ATC and the Universitat Jaume I."UKES"

6.- J. E. Enrique Navarro and E. Monfort, "Situación actual y perspectivas de futuro de los residuos de la industria azulejera", III Congreso Nacional de Técnico Cerámico, Asociación Española de Técnicos Cerámicos, Castellón, 25-27 October, 1995.

7.- G. Monrós Tomás, "Reutilización de residuos en la industria cerámica y litosíntesis cerámica", III Congreso Nacional de Técnico Cerámico, Asociación Española de Técnicos Cerámicos, Castellón, 25-27 October, 1995.

8.- J. M. Fernández Navarro, "El Vidrio", publ. Consejo Superior de Investigaciones Científicas", Madrid 1985.

9.- J. M. Rincón and A. Durán, "Separación de fases en vidrios. El sistema $\text{Na}_2\text{O}-\text{B}_2\text{O}_3-\text{SiO}_2$ ", publ. Sociedad Española de Cerámica y Vidrio, Monografías, Arganda del Rey, Madrid, 1982.

10.- "Third Euro-Ceramics, ECERS". Proceedings of the IIIrd European Ceramics Congress, Madrid 1993.P. Durán and J. F. Fernández, publ. Faenza Editrice Ibérica y Sociedad Española de Cerámica y Vidrio, Madrid 1993.

11.- "Relación entre la Estructura y las Propiedades de los Materiales". M. I. Ariortua, J. L. Pizarro and M. K. Urtiaga, publ. Universidad del País Vasco. Bilbao, 1994."ESUK"

12.- "Glasses and Glass-Ceramics for Nuclear Waste Management", J. M. Rincón, publ. Sociedad Española de Cerámica y Vidrio, 2nd edition, Madrid, 1991.

13.- J. M. Rincón. "Principles of Nucleation and Controlled Crystallisation of Glasses", Poly.-Plast. Technol. Eng., 31 (3 & 4), 309-357, 1992.

14.- P. W. Mc Millan, "Glass-Ceramics", De. Academic Press, 2nd edition, New York, London, 1979."UKES"

15.- I. de Vicente-Mingarro, P. Callejas and J. M. Rincón, "Materiales Vitrocerámicos: EL proceso Vitrocerámico", Bol. Soc. Esp. Cerm. Vidr., 32, 3, 157-167 1993.

ACKNOWLEDGEMENTS

The authors wish to express their gratitude for the facilities provided by the Electron Microscopy Service of the Universidad Politécnica de Valencia, Faenza Editrice Ibérica and AS&A Design and to Isaac Nebot.